Environmental Science & Technology
pubs.acs.org/est
Article

Global Phosphorus Losses from Croplands under Future Precipitation Scenarios

Wenfeng Liu,* Philippe Ciais, Xingcai Liu, Hong Yang, Arjen Y. Hoekstra, Qiuhong Tang, Xuhui Wang, Xiaodong Li, and Lei Cheng

Cite This: https://dx.doi.org/10.1021/acs.est.0c03978 Read Online

ABSTRACT: Phosphorus (P) losses from fertilized croplands to inland water bodies cause serious environmental problems. During wet years, high precipitation disproportionately contributes to P losses. We combine simulations of a gridded crop model and outputs from a number of hydrological and climate models to assess global impacts of changes in precipitation regimes on P losses during the 21st century. Under the baseline climate during 1991−2010, median P losses are 2.7 ± 0.5 kg P ha^{-1} year^{-1} over global croplands of four major crops, while during wet years, P losses are 3.6 ± 0.7 kg P ha^{-1} year^{-1}. By the end of this century, P losses in wet years would reach 4.2 ± 1.0 (RCP2.6) and 4.7 ± 1.3 (RCP8.5) kg P ha^{-1} year^{-1} due to increases in high annual precipitation alone. The increases in P losses are the highest (up to 200%) in the arid regions of Middle East, Central Asia, and northern Africa. Consequently, in three quarters of the world's river basins, representing about 40% of total global runoff and home up to 7 billion people, P dilution capacity of freshwater could be exceeded due to P losses from croplands by the end of this century.

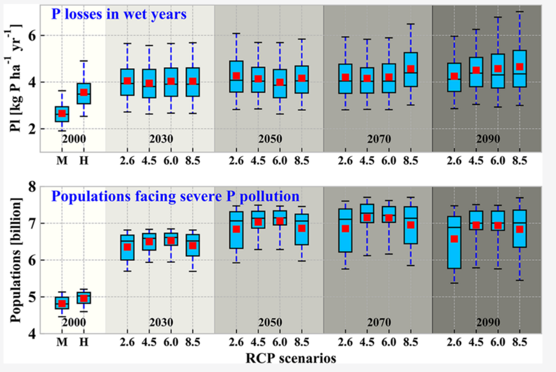

1. INTRODUCTION

Losses of phosphorus (P) from croplands to aquifers, streams, lakes, and finally oceans have resulted in severe environmental consequences around the world,[1] such as emerging eutrophication[2] and spreading anoxic dead zones in the coastal ocean.[3] P losses are projected to increase from croplands,[4,5] with more fertilizers needed to sustain a higher food production.[6] P losses are also sensitive to climatic factors, particularly changes in precipitation regimes.[7,8] To keep P loads below critical regional and global boundaries,[9] it is necessary to quantify and understand the interaction between precipitation regimes and P losses from fertilized croplands.

Under global climate change, increasing frequency and magnitude of high precipitation are projected,[10−12] which could be an important driver of P losses in intensive cultivation areas in the future. Michalak[13] outlined the overlooked impact of (increasing) climate extremes on water quality, especially for intensified P and nitrogen (N) losses. Ockenden et al.[14] found that precipitation had a strong effect on P losses and future climate (mainly precipitation) alone would increase winter P loads up to 30% by 2050 in three catchments in the U.K. Using P load measurements in two tributaries of Lake Mendota in the U.S., Carpenter et al.[15] found that precipitation extremes were associated with extremes of discharge and substantial increases in P loads. In the same region, Motew et al.[16] applied a process-based watershed model to detect the impacts of P inputs and precipitation on P loads and found a significant and positive relationship between these two factors and P concentration in water bodies. On the one hand, an increase in the balance between precipitation and evapotranspiration causes higher runoff, and this process will dilute P pollution. On the other hand, higher precipitation will increase the intensity of P losses from croplands (e.g., Carpenter et al.[15]). It is thus the balance between these two mechanisms that determines how P pollution will change with precipitation in the future. So far, studies on the influence of precipitation changes on P losses related to agriculture have only been conducted in a few specific watersheds.[14−16] Examining future P losses based on the projections from the General Circulation Models (GCMs) under different climate scenarios is still missing on a global scale. Further, previous studies did not provide quantitative estimates of exposed populations to degraded water quality across different catchments throughout the world.

The objectives of this study are to project regional P losses on the global scale from croplands in future wet years and to determine whether increased runoff in wet years is sufficient to

Received: June 17, 2020
Revised: September 6, 2020
Accepted: October 23, 2020

dilute increased P loads. We estimated global P losses by fitting a linear substitute model trained to reproduce the simulation outputs of the process-based PEPIC crop model.[17,18] Then, the substitute model was used to detect the impacts of future precipitation in wet years on annual P losses. The concept of gray water footprint (GWF)[19] was used to investigate the water pollution induced by P losses. We quantified the amount of freshwater required to dilute P pollution below a critical concentration threshold of 0.02 mg P L^{-1} based on the GWF guideline.[20] Then, the gray water stress (GWS) was calculated to indicate water P pollution levels.[21,22] We focused on the detection of regions where GWS will reach above 1, meaning that local water resources are insufficient to dilute the P loads,[21] and assessed the number of people exposed to severe P pollution. This study, which shows the validity of a linear substitute model to estimate the impacts of future precipitation in wet year on P losses, helps quantify the regional mechanisms that determine how P loads will change with precipitation under climate change.

2. MATERIALS AND METHODS

2.1. Simulation of Phosphorus Losses. In this study, P losses were defined as losses of P from croplands entrained with surface runoff and leaching water as well as soil erosion as particulate forms. All three processes were estimated by the PEPIC model[18] at a resolution of 0.5 arc degree. PEPIC is a grid-based version of the Environmental Policy Integrated Climate (EPIC) model[23] coded under the Python environment. It performed well in simulating crop yields, crop water use, and N dynamics at large scales.[18,24,25] More recently, PEPIC was successfully used to assess global P losses by conducting an integrative crop-soil-management modeling approach.[17] The ratio of simulated P losses by PEPIC to P inputs is in the middle range of previous studies and regional P losses estimated by PEPIC matched well with reported data (see Table 2 and Table S8 in the study of Liu et al.[17]). In addition, PEPIC showed a good ability in representing interannual variation of crop yields between 1980 and 2010 at the country level among 14 large-scale crop models[26,27] participating in the Agricultural Model Intercomparison and Improvement Project (AgMIP).[28] In this study, we used the verified PEPIC model to estimate P losses. Detailed information on the PEPIC model and estimation of P losses can be found in the Supporting Information.

The PEPIC model was run 100 times for each crop using 100 sets of parameter combinations to investigate uncertainties associated with model parameters. We carefully chose 19 model parameters (related to crop growth, water balance, and N, P, and carbon routines) and their possible ranges based on Wang et al.[29] and the EPIC user's manual[30] (Table S1). Parameter sampling was conducted by applying the Latin hypercube sampling method.[31,32] These parameters and sampling method were used in our previous study.[17]

Four major crops, i.e., maize, rice, soybean, and wheat, were included in this study. P fertilizer consumption for these four crops together accounts for 73% of total P fertilizers among 17 most commonly produced crops.[33] P inputs from chemical fertilizer and manure were applied along with tillage before crop planting, consistent with widely used P application methods.[34] P losses for each grid were estimated as average P losses weighted by cropland areas of the four crops. P losses at the river basin level were aggregated by using area-weighted average over cropland in the river basin. It deserves to note that the basin-scale P losses defined here are the direct losses without considering any biochemical processed of P in water bodies. The estimated P loads could be higher than delivered P from the outlet of a given basin. Here, the river basin map was derived from the FAO GeoNetwork (http://www.fao.org/geonetwork/srv/en/metadata.show?id=38047), consisting of 228 watersheds in total. P losses in the basins with the smallest cropland areas (for a total of 0.1% of global total cropland areas of the four crops) were not considered in the analysis.

2.2. Projection of Future Trend in P Losses. PEPIC simulates P losses given the precipitation and other climate variables through a set of complex equations controlling the water balance of the soil and its P budget. As runoff is roughly proportional to P losses and runoff is related to precipitation (and evapotranspiration), one can expect a positive correlation between P losses and precipitation. We developed a linear substitute model by regressing modeled P losses from each of 100 simulations against precipitation at the annual level during the baseline period 1991−2010 for each river basin, according to

$$\ln(\mathrm{Pl}) = \mathrm{slope} \times \ln(\mathrm{pr}) + \mathrm{intercept} \tag{1}$$

where Pl is the time series of total annual P losses (kg P ha^{-1} $year^{-1}$) averaged from all the cropland grid cells in each river basin (188 basins considered here) over the croplands; ln is natural log transformation, which is used to consider the possible nonlinear relationship between P losses and precipitation;[35] pr is the time series of annual precipitation (mm $year^{-1}$), which was estimated as an area-weighted average of precipitation according to the cropland fraction of each grid cell; and slope [ln(kg P ha^{-1} mm^{-1})] and intercept [ln(kg P ha^{-1} $year^{-1}$)] are model parameters. The slope presents the response of ln(Pl) to one unit change of ln(pr) over the river basin considered. It also indicates the elasticity of P losses to precipitation, i.e., 1% of change in precipitation corresponding to slope% of change in P losses. The coefficient of correlation (r) and p value by the Student t-test were used to detect the significance of the relationship.

To determine the impacts of high annual precipitation (during wet years) on P losses, we calculated the median values of P losses during the wet years (P losses of high precipitation, referred to as $\mathrm{Pl}_{h,2000}$) and the median P losses (referred to as $\mathrm{Pl}_{m,2000}$) during all the years in the period 1991−2010 (referred to as subscript 2000). Wet years are defined as the years with annual precipitation above the 75th percentile of the whole distribution in a given period. Then, the differences between $\mathrm{Pl}_{h,2000}$ and $\mathrm{Pl}_{m,2000}$ were treated as the additional P losses due to high annual precipitation. We then regressed $\ln(\mathrm{Pl}_{h,2000}) - \ln(\mathrm{Pl}_{m,2000})$ against slope × $(\ln(\mathrm{pr}_{h,2000}) - \ln(\mathrm{pr}_{m,2000}))$, where $\mathrm{pr}_{h,2000}$ and $\mathrm{pr}_{m,2000}$ are the high and median precipitation in the baseline period, to see whether it is appropriate to use the linear substitute model to detect the impacts of high precipitation on P losses as

$$\ln(\mathrm{Pl}_{h,2000}) - \ln(\mathrm{Pl}_{m,2000}) = a_h \times \mathrm{slope} \times [\ln(\mathrm{pr}_{h,2000}) - \ln(\mathrm{pr}_{m,2000})] \tag{2}$$

where a_h is the regression parameter. In addition to the comparison for high P losses, we also investigated the agreement for maximum P losses and minimum P losses as

https://dx.doi.org/10.1021/acs.est.0c03978
Environ. Sci. Technol. XXXX, XXX, XXX−XXX

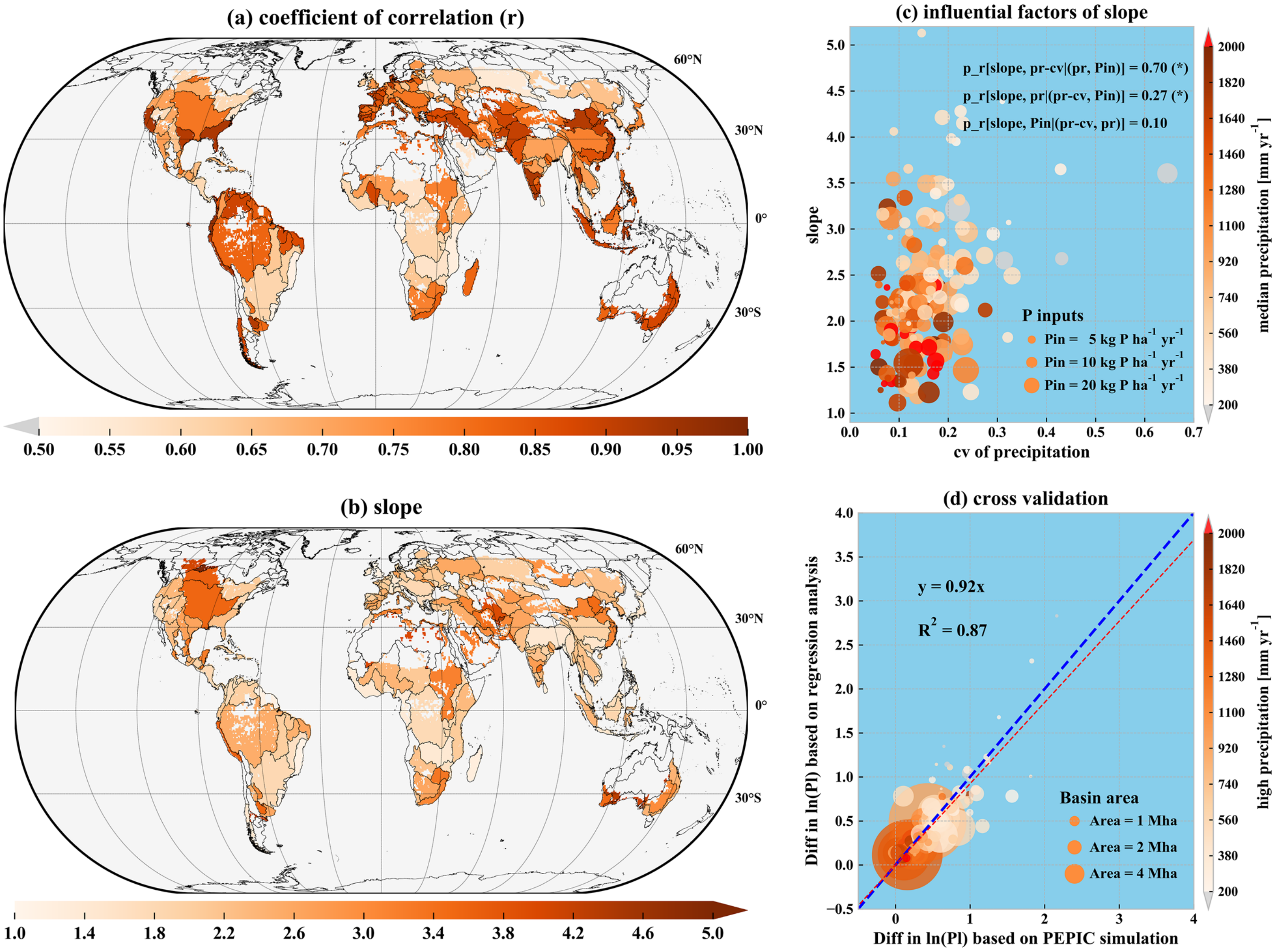

Figure 1. Relationship between natural log-transformed phosphorus losses (ln(Pl)) and natural log-transformed annual precipitation (ln(pr)) at the river basin level. (a) Coefficient of correlation (r) of the linear substitute model between ln(Pl) and ln(pr) for the period 1991−2010. (b) Slope [ln(kg P ha^{-1} mm^{-1})] of the linear substitute model. (c) Influential factors of the slope. (d) Comparison of differences in ln(Pl) (losses during the wet years minus the median of all years) between the fully fledged PEPIC model (x-axis) and the linear substitute model (y-axis). In the plot, basins with the smallest areas (for a total of 0.1% of global total cropland areas) and numbers of simulations with significant relations ($p < 0.05$) between ln(Pl) and ln(pr) lower than 50 are discarded. In subplot (c), p_r[slope, pr-cv|(pr, Pin)] is the spatial partial correlation coefficient across basins between the slope and coefficient of variation of pr (pr-cv) when controlling pr and P inputs (Pin), p_r[slope, pr|(pr-cv, Pin)] is the spatial partial correlation coefficient between slope and pr when controlling pr-cv and Pin, and p_r[slope, Pin|(pr-cv, pr)] is the spatial partial correlation coefficient between slope and Pin when controlling pr-cv and pr. In subplot (d), the equation represents the linear relationship of the dashed red line, R^2 is the coefficient of determination of the equation, and the dashed blue line is the 1:1 line.

$$\ln(\mathrm{Pl}_{\mathrm{max},2000}) - \ln(\mathrm{Pl}_{\mathrm{m},2000}) = a_{\mathrm{max}} \times \mathrm{slope} \times [\ln(\mathrm{pr}_{\mathrm{max},2000}) - \ln(\mathrm{pr}_{\mathrm{m},2000})] \tag{3}$$

$$\ln(\mathrm{Pl}_{\mathrm{m},2000}) - \ln(\mathrm{Pl}_{\mathrm{min},2000}) = a_{\mathrm{min}} \times \mathrm{slope} \times [\ln(\mathrm{pr}_{\mathrm{m},2000}) - \ln(\mathrm{pr}_{\mathrm{min},2000})] \tag{4}$$

where $\mathrm{Pl}_{\mathrm{max},2000}$ and $\mathrm{Pl}_{\mathrm{min},2000}$ are P losses in the year with maximum ($\mathrm{pr}_{\mathrm{max},2000}$) and minimum ($\mathrm{pr}_{\mathrm{min},2000}$) baseline precipitation, respectively; a_{max} and a_{min} are model fitted parameters. The robustness of relationships expressed in eqs 2−4 was detected by the coefficient of determination (R^2) and p value. The results suggested quite good performance (Figure 1d and Figure S1). In addition, we found that the slopes derived from eq 1 are mainly influenced by the coefficient of variation (cv) of precipitation (Figure 1c), which will not change much in the future. The future precipitation in wet years generally ranges between baseline minimum and maximum precipitation (Figure S2). Therefore, we used the slope obtained from the historical regression model, assuming that the slope would not change under future climate conditions, to project the impacts of future high precipitation on P losses for four periods: 2020−2039 (referred to as subscript 2030), 2040−2059 (referred to as subscript 2050), 2060−2079 (referred to as subscript 2070), and 2080−2099 (referred to as subscript 2090).

$$\mathrm{Pl}_{\mathrm{h,future}} = \mathrm{Pl}_{\mathrm{m},2000} \times \left(\frac{\mathrm{pr}_{\mathrm{h,future}}}{\mathrm{pr}_{\mathrm{m},2000}}\right)^{\mathrm{slope}} \tag{5}$$

where $\mathrm{Pl}_{\mathrm{h,future}}$ is the future P losses of high precipitation (kg P ha^{-1} year^{-1}), slope is derived from eq 1, and $\mathrm{pr}_{\mathrm{h,future}}$ is the high precipitation in the four future periods (mm year^{-1}). Equation 5 was only applied to river basins where the numbers of

https://dx.doi.org/10.1021/acs.est.0c03978
Environ. Sci. Technol. XXXX, XXX, XXX−XXX

simulations with significant ($p < 0.05$) linear relationship between ln(Pl) and ln(pr) are more than 50 out of 100, while for the other basins (responsible for only about 2% of global croplands of the four crops), $Pl_{h,future}$ was kept the same as $Pl_{h,2000}$.

To examine whether the linear substitute model performs well in representing the original PEPIC-simulated P losses under future climate conditions, we also ran the PEPIC model forced by future climate data in eight major river basins around the world. For simplicity, only two Representative Concentration Pathway (RCP) scenarios, RCP2.6 and RCP8.5, were considered for the PEPIC simulations for the periods 2030 and 2090. Then, we compared future P losses estimated by PEPIC to those estimated by the linear substitute model.

2.3. Assessment of Water Pollution Intensity Associated with Phosphorus Losses. The concepts of GWF and GWS were used to assess the water pollution intensity due to P losses into water bodies. GWF was introduced by Hoekstra et al.[19] and it measures the water requirements to dilute pollutants (P losses in this study) based on ambient water quality standard and natural background concentration. It is estimated as

$$\mathrm{GWF} = 100 \cdot \mathrm{Pl}/(C_{max} - C_{nat}) \quad (6)$$

where GWF is the gray water footprint over cropland (mm year^{-1}) associated with P losses, and C_{max} and C_{nat} (mg P L^{-1}) are the ambient water quality standard and natural background concentration of P, respectively. According to the GWF concept, the range between C_{nat} and C_{max} defines the dilution capacity of a unit of freshwater. The values of C_{max} and C_{nat} were selected as 0.02 and 0.01 mg P L^{-1} according to the GWF accounting guideline.[20] These values were also used by Mekonnen and Hoekstra.[22] The GWS was calculated as a dimensionless ratio of GWF to runoff volumes simulated by large-scale hydrological models (HMs), indicating to which level the dilution capacity of freshwater has been consumed by pollutants.[21,22] Here, GWF is over cropland, while runoff is over terrestrial land. Hence, GWF is scaled by a ratio of cropland area to terrestrial land area for each river basin. With this concept, GWS > 1 means that freshwater has exhausted the dilution capacity of a given pollutant. Therefore, we focused on the regions with GWS greater than 1 to explore to what extent land and runoff would face severe P pollution conditions and how many people would be exposed to the pollution for both the baseline situation (2000) and future conditions (2030, 2050, 2070, and 2090). Similar to P losses, we calculated median GWF and GWS and GWF and GWS during wet years.

2.4. Data Description. Input data of PEPIC include elevation, soil, climate, fertilizer, crop calendar, and crop land use.[18] Climate data for PEPIC historical simulation were obtained from the WFDEI dataset,[36] including precipitation, temperature, wind speed, and relative humidity at a daily step. Nutrient inputs of P and N from mineral fertilizer and manure were derived from the EarthStat dataset.[33,37] Crop land use data were based on the MIRCA2000 dataset,[38] which provides irrigated and rainfed land area for 26 crop species. Detailed information of input data of PEPIC can be found in the Supporting Information.

Future annual precipitation data (2020−2099) were downloaded from the data archive of the Inter-Sectoral Impact Model Intercomparison Project (ISIMIP, https://www.isimip.org/).[39] The ISIMIP climate data were derived from five CMIP5 GCMs (GFDL-ESM2M, HadGEM2-ES, IPSL-CM5A-LR, MIROC-ESM-CHEM, and NorESM1-M) under four RCP scenarios (RCP2.6, RCP4.5, RCP6.0, and RCP8.5). These precipitation data were downscaled to a resolution of 0.5° and bias-corrected with a trend-preserving method.[40] The five GCM models account for 55% of uncertainties in precipitation of the entire CMIP5 GCM models.[41] Annual runoff data were provided by four HMs, i.e., DBH,[42] H08,[43] PCR-GLOBWB,[44] and WaterGAP2.[45] These runoff data were generated for the ISIMIP fast track phase.[39] These models performed well in representing global large-scale hydrological cycles.[46] Grid-based population data for the baseline and future periods were also obtained from the ISIMIP archive, wherein the future populations were estimated based on the Shared Socioeconomic Pathway scenario 2.

In the analysis, we used the fertilizer P inputs and land use patterns at the baseline level for the future periods. As it is likely that P inputs will increase in the future in response to the higher food demand,[47] future water P pollution might be underestimated in this study.

3. RESULTS

3.1. Responses of Phosphorus Losses to Precipitation. The regression between PEPIC-simulated P losses and annual precipitation time series (both are in natural log form) shows a strong positive linear relationship across most river basins of the world (Figure 1a and Figure S3). Among the 188 river basins considered in this study, 177 of them (94%) have more than 50 simulations out of 100, presenting statistically significant positive relationships ($p < 0.05$) between ln(Pl) and ln(pr). The median coefficient of correlation (r) for simulations with significant regression relations is higher than 0.6 for 87% of the basins. The slope of the linear regression model in each river basin reflects the overall elasticity of P losses to precipitation (see Section 2). This slope shows high spatial variations and takes the highest values in the North China, central U.S., and Middle East catchments (Figure 1b). The values of the slope are mainly influenced by the cv of precipitation as the partial correlation between the slope and cv of precipitation across different catchments reaches 0.7 when controlling for P inputs and median precipitation (Figure 1c). These results indicate that a linear substitute model relating P losses to precipitation with catchment-specific slope derived from the fully fledged PEPIC simulations can explain most of the spatial variance of present-day estimated P losses.

The linear substitute model also has a good ability to reproduce year-to-year changes in P losses from precipitation, as shown by the comparison of abnormal log P losses during high annual precipitation (log of mean P losses during the 75th highest precipitation years in each catchment minus log of median P losses during all the years in the period 1991−2010) between the results from the original PEPIC model and linear substitute model (Figure 1d). In addition, the linear substitute model has a good performance for reproducing maximum minus median P losses (log form) and median minus minimum P losses (log form) from the fully fledged PEPIC (Figure S1). It also performs well in representing PEPIC estimated P losses forced by future climate data in eight major river basins throughout the world. The estimated future P losses with the linear substitute model vs with the PEPIC model were found to be comparable ($R^2 = 0.86$) between the two approaches across the eight basins (Figure S4). We noticed large standard deviation for the East Brazil basin in P

https://dx.doi.org/10.1021/acs.est.0c03978
Environ. Sci. Technol. XXXX, XXX, XXX−XXX

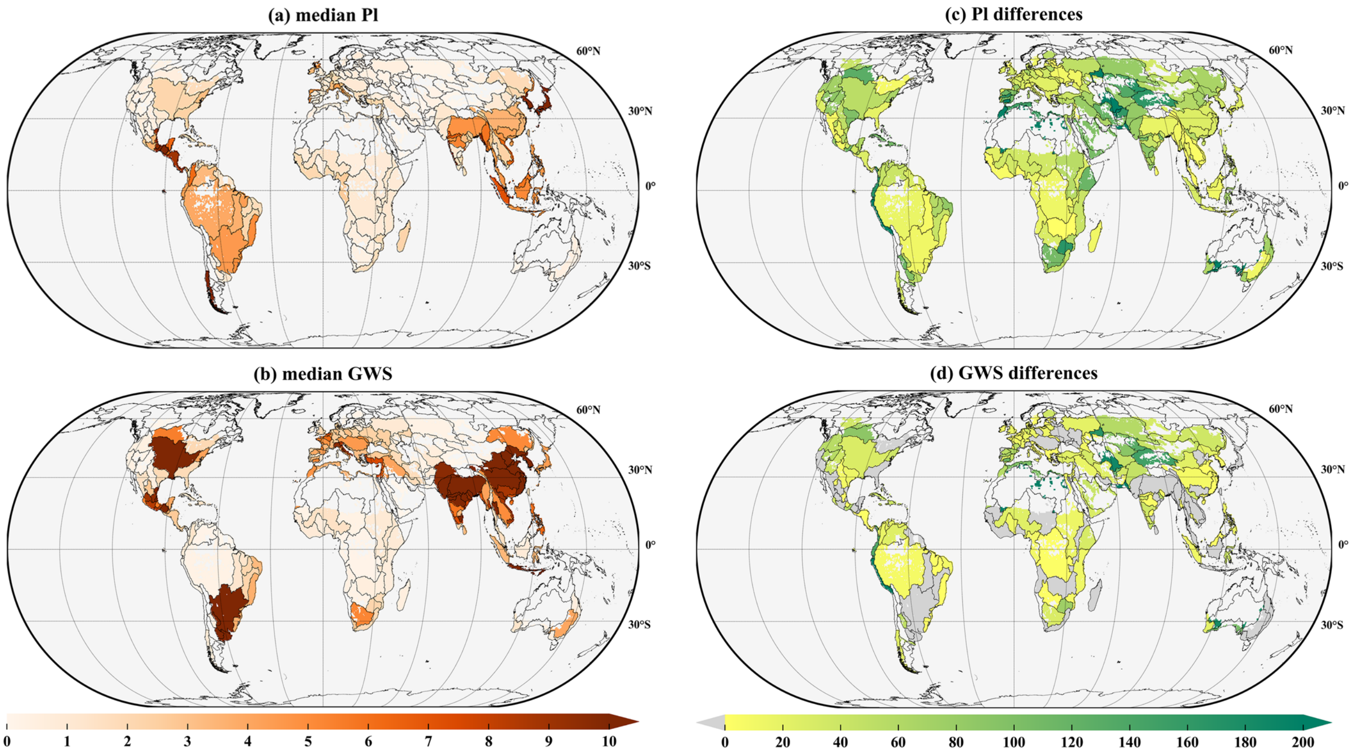

Figure 2. Impacts of high precipitation on phosphorus losses (Pl) and gray water stress (GWS) for the period 1991−2010. (a) Median Pl (kg P ha^{-1} $year^{-1}$). (b) Median GWS (dimensionless). (c) Percentage differences (%) between Pl during wet years and median Pl across all years. (d) Percentage differences (%) between GWS during wet years and median GWS across all years.

losses estimated by both methods. This is mainly because future high precipitation in this basin has much larger standard deviation across GCMs than in other basins. In addition, the level of high annual precipitation in the future generally lies in the range between baseline minimum and maximum precipitation and cv of precipitation would not change much in the future (Figure S2). This suggests that the linear substitute model calibrated on the range of baseline precipitation variability is not extrapolated outside this range when forced by future precipitation fields. In addition, the slope values for the eight river basins derived from the future simulations match well with the baseline slope values (Figure S5), which further confirms the robustness of the linear substitute model in estimating future P losses. However, the approach is based on the assumption that the interannual baseline elasticity of P losses to precipitation is conserved for each catchment under future climate conditions. It ignores, for instance, the effects of changes in precipitation frequency and intensity within a year and changes in agricultural practices and in cultivated areas from each crop type.

3.2. Effects of Baseline Phosphorus Losses on Freshwater Pollution. The baseline median annual P losses show quite similar spatial patterns as median annual precipitation at the river basin level (Figure 2a and Figure S6). That is, high P loss values occur in wet countries and regions like Japan, Korea, south-eastern China, Southeast Asia, and South America, where P inputs are also generally high. In these regions, the GWF values are extremely high, reaching over 4000 mm $year^{-1}$ in some hotspot regions, meaning that a large amount of freshwater is needed to dilute P losses (more than available when GWS > 1). About 71% (133 out of 188) of the river basins, mostly in China, India, the U.S., and Argentina, have already exceeded their dilution capacity of P pollution at the baseline level (Figure 2b).

Globally, precipitation in wet years (above the 75th percentile of all the years) is about 14% higher than median precipitation, but P losses during these wet years are 34% larger than median P losses under baseline climate (3.6 ± 0.7 (mean ± s.d.) kg P ha^{-1} $year^{-1}$ of P losses during wet years compared to 2.7 ± 0.5 kg P ha^{-1} $year^{-1}$ during median years) (Figure 3a). This disproportionate increase in global P losses relative to precipitation during wet years is mainly due to the fact that the slope values in the linear substitute model are predominantly larger than 1. Spatially, the relative increases in P losses during high vs median precipitation years are the largest in dry regions, e.g., the Middle East, Central Asia, the western U.S., northern Africa and South Africa, and southern Australia (Figure 2c). High P losses during wet years are as much as 200% higher than median P losses in some hotspot regions like the Middle East, Central Asia, and northern Africa. In these regions, the relative differences between high and median precipitation values are larger than elsewhere (Figure S6). Consequently, GWF during wet years increases strongly in these regions. The increases in P losses in most basins during wet years do not imply that the resultant GWS always increases in these basins because increased runoff also favors the dilution capacity of P pollution of freshwater. Although increases in GWS occurred in most regions in wet years, decreased values can also be observed (Figure 2d). We classified 140 river basins with GWS > 1 during wet years compared to 133 during normal (median) years. This increase (5%) in the number of basins exceeding P-thresholds in wet years suggests that large P losses occur in those basins, leading to very high pollution.

About 38 ± 4% (under normal years) and 42 ± 4% (under wet years) of global land area already experience P pollution

https://dx.doi.org/10.1021/acs.est.0c03978
Environ. Sci. Technol. XXXX, XXX, XXX−XXX

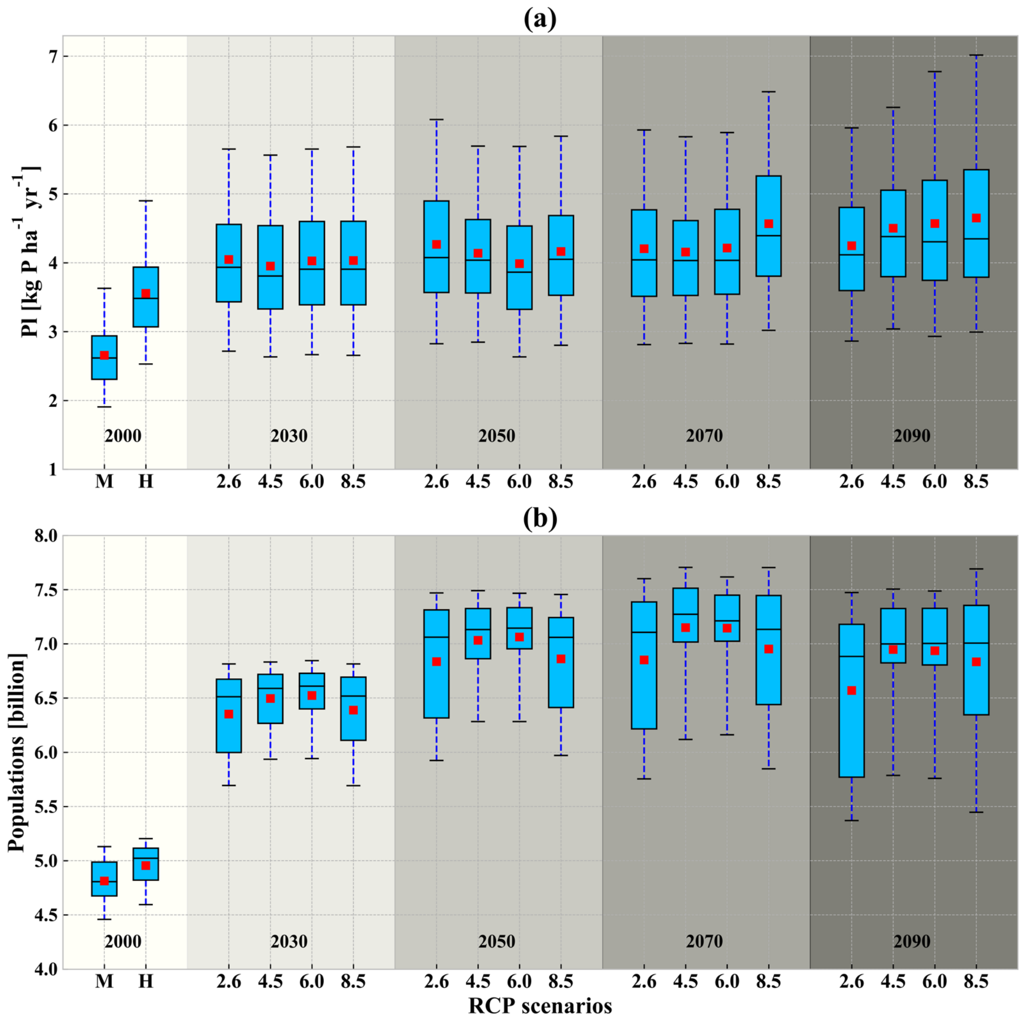

Figure 3. Responses of phosphorus losses (Pl) to high precipitation (pr) and affected popultion with gray water stress exceeding 1. (a) Median Pl and high Pl during wet years (kg P ha^{-1} year^{-1}) for the baseline period (around the year 2000) and high Pl during wet years for four future periods (2030, 2050, 2070, and 2090) and four Representative Concentration Pathway (RCP) scenarios (RCP2.6, RCP4.5, RCP6.0, and RCP8.5). (b) Total affected populations (billion). Whiskers plots give 95th, 5th, median, and interquartile values. Red square points represent mean values. M stands for median and H for high. Background colors indicate different periods.

with baseline GWS > 1 (Figure S7a). The related basins represent about 40% of total global runoff (Figure S7b). About 5 billion people are affected by polluted waters (Figure 3b).

3.3. Impacts of Future Wet Years on Freshwater Pollution. With the projected increases in high precipitation given by GCMs (Figure S8), future P losses are simulated to increase gradually from 4.0 ± 0.9 kg P ha^{-1} year^{-1} in 2030 to 4.5 ± 1.1 kg P ha^{-1} year^{-1} in 2090 (Figure 3a). Under the scenario RCP2.6, the increases in P losses are more pronounced in 2050 but less in 2070 and 2090. P losses under RCP2.6 are higher than those under the other three scenarios during the periods of 2030 and 2050, mainly due to the higher precipitation over the croplands under RCP2.6 (Figure S8). The highest global average P losses are found for 2090 under scenario RCP8.5, with losses in wet years of 4.7 ± 1.3 kg P ha^{-1} year^{-1}, which is 75 ± 48% higher than baseline median P losses and 31 ± 36% higher than baseline high P losses. Percentage increases in P losses are larger than 200% in the Middle East, north-eastern Africa, and south Asia (Figure 4a), but relative decreases are found in a few basins, e.g., northern Africa and Northwest China, where future high precipitation is lower than baseline median precipitation due to a general drying trend in these areas (Figure S2). In many basins, GWS under future high precipitation is estimated to be smaller than under baseline high precipitation (Figures 2d and 4b), holding the fertilizer inputs constant. In some regions, the GWS during wet years in 2090 will become even lower than GWS under the baseline median precipitation, e.g., in several basins in northern African, south-eastern Brazil, and Southeast Asia. These decreases in GWS are mainly due to the increases in runoff under future high precipitation to be larger in magnitude than the estimated increases in P losses, a process that dilutes P pollution. Nevertheless, GWS during the four future periods exceeds 1 in most intensively cultivated basins (Figure S9), especially in South and East Asia, West Europe, and eastern U.S., accounting for about 90% of global cropland of the four crops.

Although the land areas and runoff volumes affected with GWS > 1 are projected to increase only slightly during wet years in the future (Figure S7), the populations exposed to severe P pollution will increase from 5 billion people under baseline high precipitation to 7 billion people under future high precipitation mainly due to increases in future populations (Figure 3b). We also observed that increases in affected

https://dx.doi.org/10.1021/acs.est.0c03978
Environ. Sci. Technol. XXXX, XXX, XXX−XXX

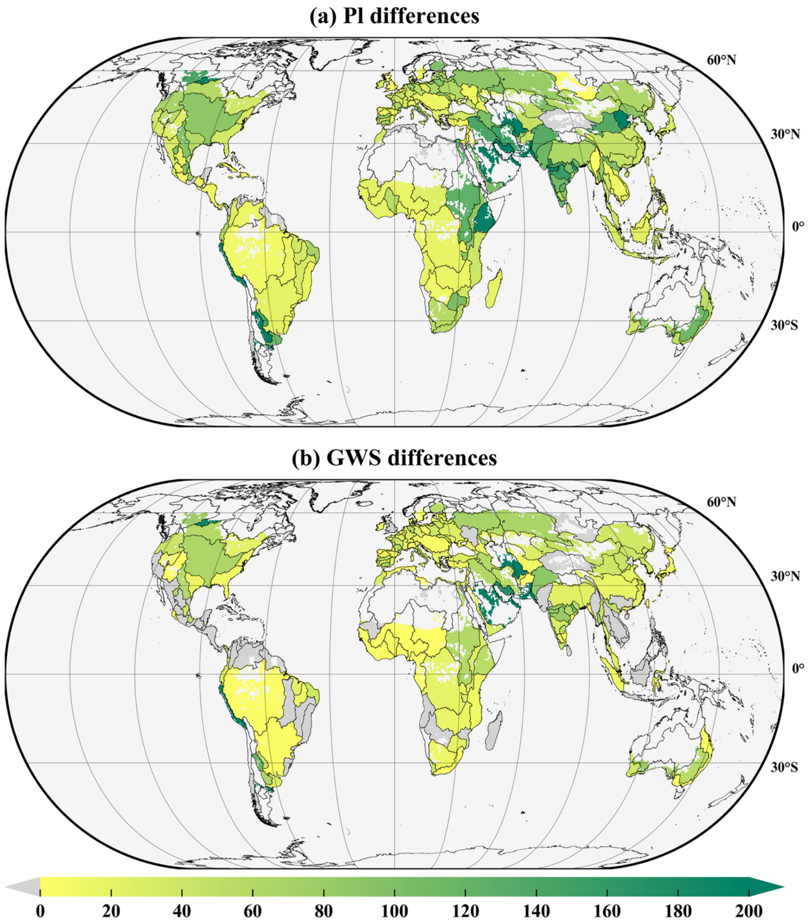

Figure 4. Relative changes in phosphorus losses (Pl) and gray water stress (GWS) in 2090 compared to baseline situation (around the year 2000). (a) Percentage differences (%) of Pl of high precipitation in 2090 in comparison to median P losses in 2000. (b) Percentage differences (%) of GWS of high precipitation in 2090 in comparison to median GWS in 2000.

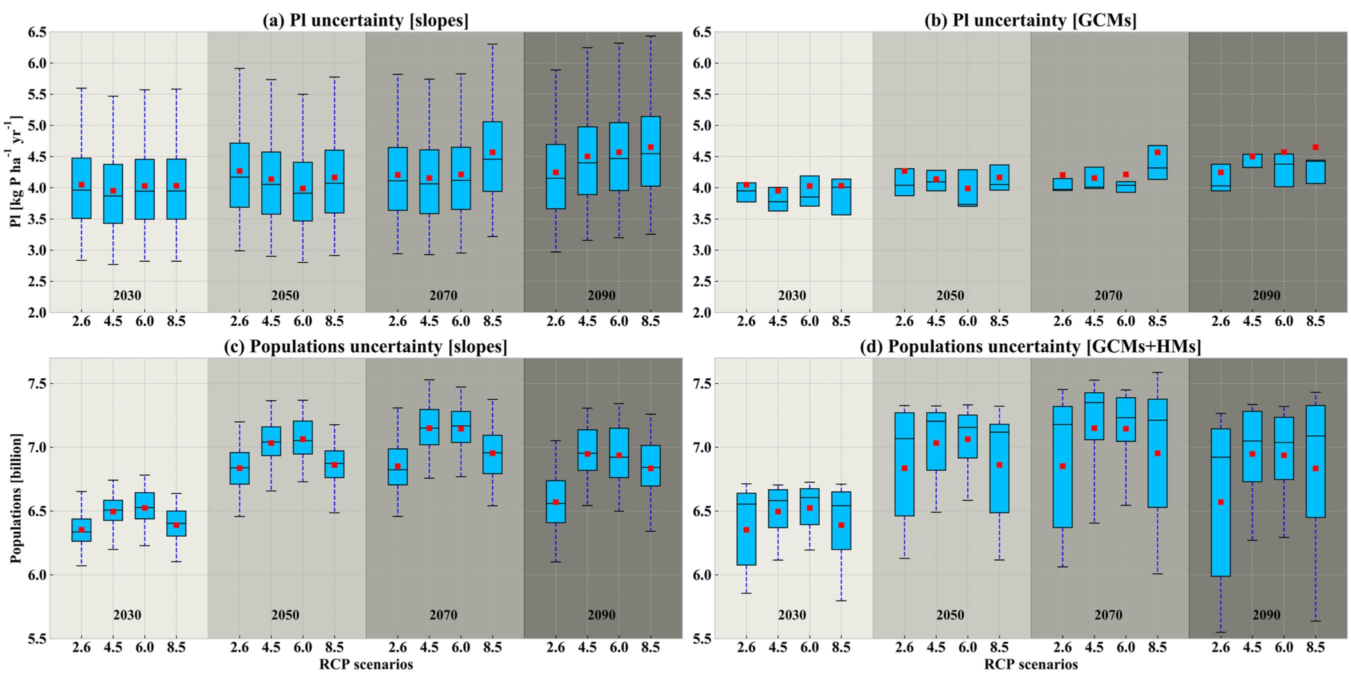

Figure 5. Uncertainties related to slopes, climate models (GCMs), and hydrological models (HMs). (a) Phosphorus losses (Pl) (kg P ha^{-1} year^{-1}) under future wet years averaged across different GCMs. (b) Pl under future wet years averaged across different slope values. (c) Affected populations (billion) with gray water stress >1 averaged across different GCMs and HMs. (d) Affected populations with gray water stress >1 averaged across different slope values.

https://dx.doi.org/10.1021/acs.est.0c03978
Environ. Sci. Technol. XXXX, XXX, XXX−XXX

populations level off after 2050 and affected populations become lower in 2090 than 2050. This is mainly because the increases in total populations are projected to slow down after 2030 and the numbers in some populous regions start to decline after 2050, e.g., in the Ganges basin in India and the Yangtze basin in China.

3.4. Uncertainty Analyses. We find that uncertainties in projecting future high P losses are more related to slope values, derived from different PEPIC parameter combinations, than different precipitation outputs from GCMs (Figure 5). As for affected populations, both slope values and combination of GCMs and HMs play an important role in the projection uncertainties. In addition to uncertainties associated with slope values, GCMs, and HMs, we also explicitly investigated the uncertainties due to the selection of different percentiles for defining wet years, that is, 65th, 70th, 75th, 80th, 85th, 90th, and 95th of the distributions of both baseline and future climates (Figure S10). A large difference in P losses during wet years can be observed when choosing varied percentiles. P losses will become higher when using a higher percentile for wet year definition, with the highest P losses reaching about 6 kg P ha^{-1} $year^{-1}$. However, there is only a minor effect on the affected populations with GWS > 1 under the different wet year definitions.

4. DISCUSSION

The impacts of high precipitation on P losses during the baseline period are the largest over dry regions with high sensitivity of P losses to precipitation, like in the Middle East, Central Asia, and the western U.S. (Figure 2b and Figure S6a). This is mainly due to high variations of precipitation, causing accumulation of P in the soil during dry years followed by high P losses during wet years in these arid regions (Figure S2). Therefore, more attention should be paid to fertilizer management in dry lands for lessening the impacts of high precipitation on P-related pollution, e.g., optimizing P application rates and timing and the types of applied P fertilizers according to crop P demand and prior soil P information, and avoiding P fertilization just after heavy rainfall events in the wet season.[48] Moreover, little freshwater is available to assimilate pollution in those dry areas, which leads to further degraded water quality. On the other hand, P losses are already high (Figure 2a) in humid regions, concurrent with high P inputs.[17] Although future high precipitation would not increase P losses that much in a relative term in these humid regions, any increase in P losses in an absolute term will further deteriorate water quality there. Interestingly, we find that future high precipitation will increase P losses, but the affected land areas and runoff with GWS > 1 will be almost consistent with baseline high precipitation conditions (Figure S7). Although future GWS in wet years would increase in many highly polluted river basins, it still stays lower than 1 in most less polluted basins as of the baseline conditions. This implies that the dilution effect of future increased runoff is comparable to the effect of a future increase in the flow of P from cropland soils to water in these less polluted basins with baseline GWS < 1. This finding holds consistent with different percentiles for defining wet years (Figure S10).

It is worth noting that the GWF concept is based on the dilution effect of freshwater, which is different from the capacity of inland water P assimilation. Although the assimilation effect was also referred in previous GWF studies,[49] it implies to account for the removal mechanisms of P in water bodies, e.g., microbial uptake, sediment burial, and sorption on mineral particles before delivery to rivers. Modeling future changes of P concentration at the outlet of a basin involves complex chemical and biological processes in the cascade of inland water. In this study, we did not model inland water P concentration changes under future climate change as it would require hydrological and biogeochemical models and knowledge to simulate the transport, burial in aquatic sediment, and reactivity of P, which is out of the scope of this study. Addressing this question should be integrated into the future development of GWF theory.

Unlike nitrate pollution, which could cause methemoglobinemia and cancers in infants,[50] high P concentration in water does not directly impair human health. However, with a growing number of people living in regions with degraded aquatic environments (e.g., dilution capacity for P will be exhausted in about three-fourths of global total river basins shown in this study), continuous P pollution will pose significant indirect impacts on human well-being.[8] A high level of precipitation will further amplify P losses under projected future climate changes, particularly in regions with high P inputs in China, India, and eastern U.S.[4] Sinha et al.[51] reported that high precipitation will increase N losses in these regions. The concurrent additional losses in P and N triggered by high precipitation could greatly challenge ecological and human health as both elements have largely transgressed their global safe planetary boundary.[52,53] In particular, P could cause more serious environmental problems due to its much lower acceptable concentrations in water bodies. Therefore, it is necessary to take urgent actions to reduce P losses, e.g., through precision farming and better nutrient management,[17,37] international food trade for improving global nutrient use efficiency,[54,55] and better P recycling and recovery.[56]

The modeling framework developed in this study provides an effective and robust tool to quantify the impacts of changing precipitation on P losses, especially in arid regions where P losses are sensitive to changes in precipitation (Figure 1b). However, the results are still subject to uncertainties. For instance, uncertainties related to fertilizer types and fertilizer data as well as application timing affect the estimation of P losses.[57] However, due to data unavailability, we had to use a simple P application method on large scale with only one global P dataset from EarthStat. We considered land use pattern unchanged for the future conditions, which may lead to underestimation of P losses because global cropland area is still growing.[58] Future work can combine our approach with variable land use scenarios. We apply the baseline relations between P losses and precipitation to estimate future P losses, which relies on future precipitation regimes only, but do not directly simulate future P losses globally based on crop modeling. Lacking future crop-specific P fertilizer information and difficulties on handling nutrient management in crop modeling for a long period[59] prevent us from doing a direct centurial simulation with PEPIC for the globe. The approach to translate future changes in high precipitation to P losses is verified for baseline precipitation regimes and several major river basins by running PEPIC with future climate, and the future contrasts between high and median precipitation are found not far out of the range from the baseline contrast values (Figure S2a). P fertilizer consumption is expected to continuously increase toward the end of this century.[60] Although this increase in P uses may not increase the

https://dx.doi.org/10.1021/acs.est.0c03978
Environ. Sci. Technol. XXXX, XXX, XXX−XXX

elasticities of P losses to annual precipitation (Figure 1c), it will certainly increase P losses.[17] We also noticed that cv of future precipitation in a few river basins is slightly different from the baseline cv (Figure S2b). This change, to some degree, could affect the projection of P losses under the future climate. Therefore, further local investigation is needed in these specific regions in future studies.

In addition to the agricultural sector, P losses from other sectors, e.g., domestic and industry, also generate P loads in inland water bodies. For instance, exposed populations with GWS > 1 increase by 0.5−1 billion (Figure S11) when considering industrial and domestic P losses obtained from Mekonnen and Hoekstra.[22] As nonagricultural P losses are with high uncertainty to project,[60] we did not consider them in this study. Instead, we isolated the impacts of precipitation changes on P losses as changes in future precipitation can hardly be avoided through local management. We focused on interannual patterns of precipitation in this study, while changing distribution on precipitation within a year will also affect P losses.[15] Therefore, investigation on the effects of P input increases and intra-annual precipitation changes on P losses should be the focus of future research. This study, for the first time, to our best knowledge, explicitly estimates the impacts of future precipitation changes on P losses and highlights the hotspot regions and associated negative consequences on a global scale. It is of particular importance to inform policy decisions for controlling P-related pollutions in the context of changing climate.

■ ASSOCIATED CONTENT

Supporting Information

The Supporting Information is available free of charge at https://pubs.acs.org/doi/10.1021/acs.est.0c03978.

> Details on model description and model parameters (supporting text and supporting tables); details on model validation, comparison of future high precipitation, and comparison of slope values between baseline and future climates; details on future high precipitation, affected land areas, and runoff with gray water stress > 1; details on spatial distribution of future gray water stress; details on uncertainties related to the percentiles for defining wet years (PDF)

■ AUTHOR INFORMATION

Corresponding Author

Wenfeng Liu − *Laboratoire des Sciences du Climat et de l'Environnement, LSCE/IPSL, CEA-CNRS-UVSQ, Université Paris-Saclay, F-91191 Gif-sur-Yvette, France; College of Water Resources and Civil Engineering, China Agricultural University, Beijing 100083, China;* orcid.org/0000-0002-8699-3677; Phone: +33 1 69 08 87 39; Email: wfliu2012@gmail.com, wenfeng.liu@lsce.ipsl.fr

Authors

Philippe Ciais − *Laboratoire des Sciences du Climat et de l'Environnement, LSCE/IPSL, CEA-CNRS-UVSQ, Université Paris-Saclay, F-91191 Gif-sur-Yvette, France*

Xingcai Liu − *Eawag, Swiss Federal Institute of Aquatic Science and Technology, CH-8600 Duebendorf, Switzerland; Key Laboratory of Water Cycle and Related Land Surface Processes, Institute of Geographic Sciences and Natural Resources Research, Chinese Academy of Sciences, Beijing 100101, China*

Hong Yang − *Eawag, Swiss Federal Institute of Aquatic Science and Technology, CH-8600 Duebendorf, Switzerland; Department of Environmental Sciences, MGU, University of Basel, CH-4003 Basel, Switzerland*

Arjen Y. Hoekstra − *Twente Water Centre, University of Twente, 7522 NB Enschede, The Netherlands; Institute of Water Policy, Lee Kuan Yew School of Public Policy, National University of Singapore, 259772, Singapore*

Qiuhong Tang − *Key Laboratory of Water Cycle and Related Land Surface Processes, Institute of Geographic Sciences and Natural Resources Research, Chinese Academy of Sciences, Beijing 100101, China; University of Chinese Academy of Sciences, Beijing 100049, China;* orcid.org/0000-0002-0886-6699

Xuhui Wang − *Laboratoire des Sciences du Climat et de l'Environnement, LSCE/IPSL, CEA-CNRS-UVSQ, Université Paris-Saclay, F-91191 Gif-sur-Yvette, France; College of Urban & Environmental Sciences, Peking University, Beijing 100871, China*

Xiaodong Li − *State Key Laboratory of Hydraulics and Mountain River Engineering, Sichuan University, 610065 Chengdu, China*

Lei Cheng − *State Key Laboratory of Water Resources and Hydropower Engineering Science, Wuhan University, Wuhan 430072, China; Hubei Provincial Collaborative Innovation Center for Water Resources Security, Wuhan 430072, China*

Complete contact information is available at: https://pubs.acs.org/10.1021/acs.est.0c03978

Author Contributions

W.L., P.C., and H.Y. designed the research. W.L. and X.L. collected the ISIMIP data. W.L. run the PEPIC model, analyzed the data, and wrote the draft. All authors participated in the interpretation of results and the writing and editing process.

Notes

The authors declare no competing financial interest.

■ ACKNOWLEDGMENTS

This work is dedicated to the memory of A.Y.H. We thank Prof. Dr. M. M. Mekonnen from the University of Nebraska for sharing datasets of domestic and industrial phosphorus losses. We are grateful to the Inter-Sectoral Impact Model Intercomparison Project (ISIMIP) for providing the climate, runoff, and population data. This study was supported by the funding from the Swiss National Science Foundation (P2EZP2_175096), the French State Aid managed by the ANR under the "Investissements d'avenir" programme with the reference ANR-16-CONV-0003, the European Research Council Synergy project SyG-2013-610028 IMBALANCE-P, and the Open Fund Research project by the State Key Laboratory of Hydraulics and Mountain River Engineering (Sichuan University) (SKHL1709). X.L. and Q.T. are supported by the Strategic Priority Research Program of Chinese Academy of Sciences (XDA20060402) and National Natural Science Foundation of China (41790424).

■ REFERENCES

(1) Chen, M.; Graedel, T. E. A half-century of global phosphorus flows, stocks, production, consumption, recycling, and environmental impacts. *Global Environ. Change* **2016**, *36*, 139−152.

(2) Carpenter, S. R. Phosphorus control is critical to mitigating eutrophication. *Proc. Natl. Acad. Sci. U. S. A.* **2008**, *105*, 11039−11040.
(3) Diaz, R. J.; Rosenberg, R. Spreading dead zones and consequences for marine ecosystems. *Science* **2008**, *321*, 926−929.
(4) Bouwman, L.; Goldewijk, K. K.; Van Der Hoek, K. W.; Beusen, A. H. W.; Van Vuuren, D. P.; Willems, J.; Rufino, M. C.; Stehfest, E. Exploring global changes in nitrogen and phosphorus cycles in agriculture induced by livestock production over the 1900-2050 period. *Proc. Natl. Acad. Sci. U. S. A* **2013**, *110*, 20882−20887.
(5) Sutton, M. A.; Bleeker, A.; Howard, C. M.; Erisman, J. W.; Abrol, Y. P.; Bekunda, M.; Datta, A.; Davidson, E.; de Vries, W.; Oenema, O.; Zhang, F. S. *Our Nutrient World: the challenge to produce more food and energy with less pollution*; Centre for Ecology and Hydrology (CEH): 2013.
(6) Tilman, D.; Balzer, C.; Hill, J.; Befort, B. L. Global food demand and the sustainable intensification of agriculture. *Proc. Natl. Acad. Sci. U. S. A.* **2011**, *108*, 20260−20264.
(7) Tong, Y.; Zhang, W.; Wang, X.; Couture, R.-M.; Larssen, T.; Zhao, Y.; Li, J.; Liang, H.; Liu, X.; Bu, X.; He, W.; Zhang, Q.; Lin, Y. Decline in Chinese lake phosphorus concentration accompanied by shift in sources since 2006. *Nat. Geosci.* **2017**, *10*, 507−511.
(8) Michalak, A. M.; Anderson, E. J.; Beletsky, D.; Boland, S.; Bosch, N. S.; Bridgeman, T. B.; Chaffin, J. D.; Cho, K.; Confesor, R.; Daloğlu, I.; DePinto, J. V.; Evans, M. A.; Fahnenstiel, G. L.; He, L.; Ho, J. C.; Jenkins, L.; Johengen, T. H.; Kuo, K. C.; LaPorte, E.; Liu, X.; McWilliams, M. R.; Moore, M. R.; Posselt, D. J.; Richards, R. P.; Scavia, D.; Steiner, A. L.; Verhamme, E.; Wright, D. M.; Zagorski, M. A. Record-setting algal bloom in Lake Erie caused by agricultural and meteorological trends consistent with expected future conditions. *Proc. Natl. Acad. Sci. U. S. A.* **2013**, *110*, 6448−6452.
(9) Elser, J.; Bennett, E. Phosphorus cycle: A broken biogeochemical cycle. *Nature* **2011**, *478*, 29−31.
(10) Fischer, E. M.; Knutti, R. Observed heavy precipitation increase confirms theory and early models. *Nat. Clim. Change* **2016**, *6*, 986−991.
(11) Stott, P. How climate change affects extreme weather events. *Science* **2016**, *352*, 1517−1518.
(12) IPCC *Managing the risks of extreme events and disasters to advance climate change adaptation*; Cambridge University Press: Cambridge, UK, and New York, NY, USA, 2012; 582.
(13) Michalak, A. M. Study role of climate change in extreme threats to water quality. *Nature* **2016**, *535*, 349−350.
(14) Ockenden, M. C.; Hollaway, M. J.; Beven, K. J.; Collins, A. L.; Evans, R.; Falloon, P. D.; Forber, K. J.; Hiscock, K. M.; Kahana, R.; Macleod, C. J. A.; Tych, W.; Villamizar, M. L.; Wearing, C.; Withers, P. J. A.; Zhou, J. G.; Barker, P. A.; Burke, S.; Freer, J. E.; Johnes, P. J.; Snell, M. A.; Surridge, B. W. J.; Haygarth, P. M. Major agricultural changes required to mitigate phosphorus losses under climate change. *Nat. Commun.* **2017**, *8*, 161.
(15) Carpenter, S. R.; Booth, E. G.; Kucharik, C. J. Extreme precipitation and phosphorus loads from two agricultural watersheds. *Limnol. Oceanogr.* **2017**, *63*, 1221−1233.
(16) Motew, M.; Booth, E. G.; Carpenter, S. R.; Chen, X.; Kucharik, C. J. The synergistic effect of manure supply and extreme precipitation on surface water quality. *Environ. Res. Lett.* **2018**, *13*, No. 044016.
(17) Liu, W.; Yang, H.; Ciais, P.; Stamm, C.; Zhao, X.; Williams, J. R.; Abbaspour, K. C.; Schulin, R. Integrative crop-soil-management modeling to assess global phosphorus losses from major crop cultivations. *Global Biogeochem. Cycles* **2018**, *32*, 1074−1086.
(18) Liu, W.; Yang, H.; Folberth, C.; Wang, X.; Luo, Q.; Schulin, R. Global investigation of impacts of PET methods on simulating crop-water relations for maize. *Agric. For. Meteorol.* **2016**, *221*, 164−175.
(19) Hoekstra, A. Y.; Chapagain, A. K.; Aldaya, M. M.; Mekonnen, M. M. *The water footprint assessment manual: Setting the global standard*; Routledge: London, UK, 2011.
(20) Franke, N. A.; Boyacioglu, H.; Hoekstra, A. Y. *Grey water footprint accounting: Tier 1 supporting guidelines*; Value of Water Research Report Series No. 65, Delft: UNESCO-IHE: The Netherlands, 2013.
(21) Liu, W.; Antonelli, M.; Liu, X.; Yang, H. Towards improvement of grey water footprint assessment: With an illustration for global maize cultivation. *J. Cleaner Prod.* **2017**, *147*, 1−9.
(22) Mekonnen, M. M.; Hoekstra, A. Y. Global anthropogenic phosphorus loads to fresh water and associated grey water footprints and water pollution levels: A high-resolution global study. *Water Resour. Res.* **2017**, *54*, 345−358.
(23) Williams, J. R.; Jones, C. A.; Dyke, P. T. A modeling approach to determining the relationship between erosion and soil productivity. *Trans. ASAE* **1984**, *27*, 129−144.
(24) Liu, W.; Yang, H.; Folberth, C.; Müller, C.; Ciais, P.; Abbaspour, K. C.; Schulin, R. Achieving high crop yields with low nitrogen emissions in global agricultural input intensification. *Environ. Sci. Technol.* **2018**, *52*, 13782−13791.
(25) Liu, W.; Yang, H.; Liu, J.; Azevedo, L. B.; Wang, X.; Xu, Z.; Abbaspour, K. C.; Schulin, R. Global assessment of nitrogen losses and trade-offs with yields from major crop cultivations. *Sci. Total Environ.* **2016**, *572*, 526−537.
(26) Müller, C.; Elliott, J.; Chryssanthacopoulos, J.; Arneth, A.; Balkovic, J.; Ciais, P.; Deryng, D.; Folberth, C.; Glotter, M.; Hoek, S.; Iizumi, T.; Izaurralde, R. C.; Jones, C.; Khabarov, N.; Lawrence, P.; Liu, W.; Olin, S.; Pugh, T. A. M.; Ray, D. K.; Reddy, A.; Rosenzweig, C.; Ruane, A. C.; Sakurai, G.; Schmid, E.; Skalsky, R.; Song, C. X.; Wang, X.; de Wit, A.; Yang, H. Global gridded crop model evaluation: benchmarking, skills, deficiencies and implications. *Geosci. Model Dev.* **2017**, *10*, 1403−1422.
(27) Porwollik, V.; Müller, C.; Elliott, J.; Chryssanthacopoulos, J.; Iizumi, T.; Ray, D. K.; Ruane, A. C.; Arneth, A.; Balkovič, J.; Ciais, P.; Deryng, D.; Folberth, C.; Izaurralde, R. C.; Jones, C. D.; Khabarov, N.; Lawrence, P. J.; Liu, W.; Pugh, T. A. M.; Reddy, A.; Sakurai, G.; Schmid, E.; Wang, X.; de Wit, A.; Wu, X. Spatial and temporal uncertainty of crop yield aggregations. *Eur. J. Agron.* **2017**, *88*, 10−21.
(28) Rosenzweig, C.; Jones, J. W.; Hatfield, J. L.; Ruane, A. C.; Boote, K. J.; Thorburn, P.; Antle, J. M.; Nelson, G. C.; Porter, C.; Janssen, S.; Asseng, S.; Basso, B.; Ewert, F.; Wallach, D.; Baigorria, G.; Winter, J. M. The Agricultural Model Intercomparison and Improvement Project (AgMIP): Protocols and pilot studies. *Agric. For. Meteorol.* **2013**, *170*, 166−182.
(29) Wang, X.; Williams, J. R.; Gassman, P. W.; Baffaut, C.; Izaurralde, R. C.; Jeong, J.; Kiniry, J. R. EPIC and APEX: Model use, calibration, and validation. *Trans. ASAE* **2012**, *55*, 1447−1462.
(30) Gerik, T.; Williams, J. R.; Dagitz, S.; Magre, M.; Meinardus, A.; Steglich, E.; Taylor, R. *EPIC User's Manual Version 0810*; Environmental Policy Integrated Climate Model: Temple, Texas, 2015.
(31) Abbaspour, K. C.; Yang, J.; Reichert, P.; Vejdani, M.; Haghighat, S.; Srinivasan, R. *SWAT-CUP: SWAT calibration and uncertaintyprograms*; Eawag: Dübendorf, Switzerland, 2011.
(32) Mckay, M. D.; Beckman, R. J.; Conover, W. J. A comparison of three methods for selecting values of input variables in the analysis of output from a computer code. *Technometrics* **2012**, *42*, 55−61.
(33) West, P. C.; Gerber, J. S.; Engstrom, P. M.; Mueller, N. D.; Brauman, K. A.; Carlson, K. M.; Cassidy, E. S.; Johnston, M.; MacDonald, G. K.; Ray, D. K.; Siebert, S. Leverage points for improving global food security and the environment. *Science* **2014**, *345*, 325−328.
(34) Elliott, J.; Müller, C.; Deryng, D.; Chryssanthacopoulos, J.; Boote, K. J.; Büchner, M.; Foster, I.; Glotter, M.; Heinke, J.; Iizumi, T.; Izaurralde, R. C.; Mueller, N. D.; Ray, D. K.; Rosenzweig, C.; Ruane, A. C.; Sheffield, J. The Global Gridded Crop Model Intercomparison: data and modeling protocols for Phase 1 (v1. 0). *Geosci. Model Dev.* **2015**, *8*, 261−277.
(35) Fu, J.; Wu, Y.; Wang, Q.; Hu, K.; Wang, S.; Zhou, M.; Hayashi, K.; Wang, H.; Zhan, X.; Jian, Y.; Cai, C.; Song, M.; Liu, K.; Wang, Y.; Zhou, F.; Zhu, J. Importance of subsurface fluxes of water, nitrogen and phosphorus from rice paddy fields relative to surface runoff. *Agric. Water Manage.* **2019**, *213*, 627−635.

https://dx.doi.org/10.1021/acs.est.0c03978
Environ. Sci. Technol. XXXX, XXX, XXX−XXX

(36) Weedon, G. P.; Balsamo, G.; Bellouin, N.; Gomes, S.; Best, M. J.; Viterbo, P. The WFDEI meteorological forcing data set: WATCH Forcing Data methodology applied to ERA-Interim reanalysis data. *Water Resour. Res.* **2014**, *50*, 7505−7514.
(37) Mueller, N. D.; Gerber, J. S.; Johnston, M.; Ray, D. K.; Ramankutty, N.; Foley, J. A. Closing yield gaps through nutrient and water management. *Nature* **2012**, *490*, 254−257.
(38) Portmann, F. T.; Siebert, S.; Döll, P. MIRCA2000-Global monthly irrigated and rainfed crop areas around the year 2000: A new high-resolution data set for agricultural and hydrological modeling. *Global Biogeochem. Cycles* **2010**, *24*, GB1011.
(39) Warszawski, L.; Frieler, K.; Huber, V.; Piontek, F.; Serdeczny, O.; Schewe, J. The Inter-Sectoral Impact Model Intercomparison Project (ISI-MIP): Project framework. *Proc. Natl. Acad. Sci. U. S. A.* **2014**, *111*, 3228−3232.
(40) Hempel, S.; Frieler, K.; Warszawski, L.; Schewe, J.; Piontek, F. A trend-preserving bias correction-the ISI-MIP approach. *Earth Syst. Dyn.* **2013**, *4*, 219−236.
(41) McSweeney, C. F.; Jones, R. G. How representative is the spread of climate projections from the 5 CMIP5 GCMs used in ISI-MIP? *Clim. Serv.* **2016**, *1*, 24−29.
(42) Tang, Q.; Oki, T.; Kanae, S.; Hu, H. The influence of precipitation variability and partial irrigation within grid cells on a hydrological simulation. *J. Hydrometeorology* **2007**, *8*, 499−512.
(43) Hanasaki, N.; Yoshikawa, S.; Pokhrel, Y.; Kanae, S. A global hydrological simulation to specify the sources of water used by humans. *Hydrol. Earth Syst. Sci.* **2018**, *22*, 789−817.
(44) Wada, Y.; Wisser, D.; Bierkens, M. F. P. Global modeling of withdrawal, allocation and consumptive use of surface water and groundwater resources. *Earth Syst. Dyn.* **2014**, *5*, 15−40.
(45) Müller Schmied, H.; Adam, L.; Eisner, S.; Fink, G.; Flörke, M.; Kim, H.; Oki, T.; Portmann, F. T.; Reinecke, R.; Riedel, C.; Song, Q.; Zhang, J.; Doll, P. Variations of global and continental water balance components as impacted by climate forcing uncertainty and human water use. *Hydrol. Earth Syst. Sci.* **2016**, *20*, 2877−2898.
(46) Schewe, J.; Heinke, J.; Gerten, D.; Haddeland, I.; Arnell, N. W.; Clark, D. B.; Dankers, R.; Eisner, S.; Fekete, B. M.; Colón-González, F. J.; Gosling, S. N.; Kim, H.; Liu, X.; Masaki, Y.; Portmann, F. T.; Satoh, Y.; Stacke, T.; Tang, Q.; Wada, Y.; Wisser, D.; Albrecht, T.; Frieler, K.; Piontek, F.; Warszawski, L.; Kabat, P. Multimodel assessment of water scarcity under climate change. *Proc. Natl. Acad. Sci. U. S. A.* **2014**, *111*, 3245−3250.
(47) Mogollón, J. M.; Beusen, A. H. W.; van Grinsven, H. J. M.; Westhoek, H.; Bouwman, A. F. Future agricultural phosphorus demand according to the shared socioeconomic pathways. *Global Environ. Change* **2018**, *50*, 149−163.
(48) Bindraban, P. S.; Dimkpa, C. O.; Pandey, R. Exploring phosphorus fertilizers and fertilization strategies for improved human and environmental health. *Biol. Fertil. Soils* **2020**, *56*, 299−317.
(49) Zhi, Y.; Yang, Z.; Yin, X.; Hamilton, P. B.; Zhang, L. Using gray water footprint to verify economic sectors' consumption of assimilative capacity in a river basin: model and a case study in the Haihe River Basin, China. *J. Cleaner Prod.* **2015**, *92*, 267−273.
(50) Ward, M. H.; Jones, R. R.; Brender, J. D.; de Kok, T. M.; Weyer, P. J.; Nolan, B. T.; Villanueva, C. M.; van Breda, S. G. Drinking water nitrate and human health: An updated review. *Int. J. Environ. Res. Public Health* **2018**, *15*, 1557.
(51) Sinha, E.; Michalak, A. M.; Balaji, V. Eutrophication will increase during the 21st century as a result of precipitation changes. *Science* **2017**, *357*, 405−408.
(52) Carpenter, S. R.; Bennett, E. M. Reconsideration of the planetary boundary for phosphorus. *Environ. Res. Lett.* **2011**, *6*, No. 014009.
(53) Rockström, J.; Steffen, W.; Noone, K.; Persson, Å.; Chapin, F. S., III; Lambin, E. F.; Lenton, T. M.; Scheffer, M.; Folke, C.; Schellnhuber, H. J.; Nykvist, B.; de Wit, C. A.; Hughes, T.; van der Leeuw, S.; Rodhe, H.; Sörlin, S.; Snyder, P. K.; Costanza, R.; Svedin, U.; Falkenmark, M.; Karlberg, L.; Corell, R. W.; Fabry, V. J.; Hansen, J.; Walker, B.; Liverman, D.; Richardson, K.; Crutzen, P.; Foley, J. A. A safe operating space for humanity. *Nature* **2009**, *461*, 472−475.
(54) Liu, W.; Yang, H.; Liu, Y.; Kummu, M.; Hoekstra, A. Y.; Liu, J.; Schulin, R. Water resources conservation and nitrogen pollution reduction under global food trade and agricultural intensification. *Sci. Total Environ.* **2018**, *633*, 1591−1601.
(55) Lassaletta, L.; Billen, G.; Garnier, J.; Bouwman, L.; Velazquez, E.; Mueller, N. D.; Gerber, J. S. Nitrogen use in the global food system: past trends and future trajectories of agronomic performance, pollution, trade, and dietary demand. *Environ. Res. Lett.* **2016**, *11*, No. 095007.
(56) Powers, S. M.; Chowdhury, R. B.; MacDonald, G. K.; Metson, G. S.; Beusen, A. H. W.; Bouwman, A. F.; Hampton, S. E.; Mayer, B. K.; McCrackin, M. L.; Vaccari, D. A. Global opportunities to increase agricultural independence through phosphorus recycling. *Earth's Future* **2019**, *7*, 370−383.
(57) Wang, Q.; Zhou, F.; Shang, Z.; Ciais, P.; Winiwarter, W.; Jackson, R. B.; Tubiello, F. N.; Janssens-Maenhout, G.; Tian, H.; Cui, X.; Canadell, J. G.; Piao, S.; Tao, S. Data-driven estimates of global nitrous oxide emissions from croplands. *Natl. Sci. Rev.* **2020**, *7*, 441−452.
(58) *The future of food and agriculture − Alternative pathways to 2050*; Food and Agriculture Organization: 2018; p 224.
(59) Folberth, C.; Gaiser, T.; Abbaspour, K. C.; Schulin, R.; Yang, H. Regionalization of a large-scale crop growth model for sub-Saharan Africa: Model setup, evaluation, and estimation of maize yields. *Agric., Ecosyst. Environ.* **2012**, *151*, 21−33.
(60) Van Vuuren, D. P.; Bouwman, A. F.; Beusen, A. H. W. Phosphorus demand for the 1970-2100 period: A scenario analysis of resource depletion. *Global Environ. Change* **2010**, *20*, 428−439.

https://dx.doi.org/10.1021/acs.est.0c03978
Environ. Sci. Technol. XXXX, XXX, XXX−XXX